Outward Current in Single Smooth Muscle Cells of the Guinea Pig Taenia Coli

Y. YAMAMOTO, S. L. HU, and C. Y. KAO

From the Department of Pharmacology, State University of New York Downstate Medical Center, Brooklyn, New York 11203

ABSTRACT   In single myocytes of the guinea pig taenia coli, dispersed by enzymatic digestion, the late outward current is carried by K^+. It has both a Ca^{2+}-activated component and a voltage-dependent component which is resistant to external Co^{2+}. The reversal potential is -84 mV, and the channel(s) for it are highly selective to K^+. At 33°C, the activation follows n^2 kinetics, with a voltage-dependent time constant of 10.6 ms at 0 mV, which shortens to 1.7 ms at $+70$ mV. Deactivation follows a single-exponential time course, with a voltage-dependent time constant of 11 ms at -50 mV, which lengthens to 33 ms at -20 mV. During a 4.5-s maintained depolarization, I_K inactivates, most of it into two exponential components, but there is a small noninactivating residue. It is surmised that during an action potential under physiological conditions, there is sufficient I_K to cause repolarization.

INTRODUCTION

This paper deals with the outward current in single smooth muscle cells enzymatically dissociated from the guinea pig taenia coli. The general features of the ionic currents in this cell as well as its inward current have been covered in a previous paper (Yamamoto et al., 1989). The early, transient inward current in the guinea pig taenia coli is carried by Ca^{2+} (Inomata and Kao, 1976; Yamamoto et al., 1989). In earlier studies using multicellular preparations (Inomata and Kao, 1976, 1979, 1985), it has been shown that the late outward current is carried by K^+, and that a component of it is Ca^{2+} activated. Results in this paper will deal in greater detail with these issues as well as provide information on certain kinetic properties of K^+ channels that could not be investigated previously.

MATERIAL AND METHODS

Isolation of single cells and voltage clamping in the whole-cell mode using the tight-seal method have been described in detail (Yamamoto et al., 1989). The composition of the vari-

ous solutions used are given in Table I of that paper. Specifically, solutions B, C, D, and F were used in the bath, and either a K^+ or Cs^+ solution was used in the pipette.

RESULTS

Outward Current

To isolate the outward current for detailed study, we have generally used 5 mM Co^{2+} to block the I_{Ca} (Yamamoto et al., 1989). However, the procedure is not entirely innocuous: because of the presence of a component of Ca^{2+}-activated I_K in these cells, total I_K is somewhat reduced whenever Ca^{2+} influx is reduced, and Co^{2+} itself could have a small direct effect on the K^+ channel. An alternative is to use a Ca^{2+}-free medium in which no inward current occurs (Yamamoto et al., 1989). There are worse complicating factors with this method. In a Ca^{2+}-free medium, an outward current (apparently carried by Cs^+ from the pipette solution) moves through the Ca^{2+} channel, which begins at as low as +40 mV, and which can be quite sizable (Fig. 8 of Yamamoto et al., 1989). Such a current would seriously interfere with any study of the I_K. A similar outward current occurs in the Co^{2+}-treated cell, but its magnitude is much smaller. Therefore, unavoidable as the error is, it is smaller than that in the case of a Ca^{2+}-free medium. Because of these limitations, we used Co^{2+} in spite of a small systematic error caused by the slight reduction of I_K. Fig. 1 illustrates this point, as well as the ready reversibility of the effect on the outward current when Co^{2+} was removed. It migth be noted that the reversibility of the effect on I_K is rather complete, even when I_{Ca} is only partially recovered. This partial recovery could be due to some residual effect of Co^{2+} or to some rundown of the Ca^{2+} channel.

Reversal potential and identity of the charge carrier. In five cells bathed in Krebs' solution (solution B, Table I of Yamamoto et al., 1989, containing 5.4 mM K^+ and 1 mM Ca^{2+}) that were voltage clamped, using electrodes containing 144 mM K^+ (Table II, Yamamoto et al., 1989), the reversal potential of the outward current was determined by tail current analysis (Fig. 2). A 50-ms step to +50 mV was used to activate both the early Ca^{2+} channel and the K^+ channel. The cell was then repolarized to different voltages to elicit tail currents. The activating step was long enough to fully inactivate the fast I_{Ca}. However, a small amount of the more slowly inactivating I_{Ca}'s might still be present at 50 ms (Yamamoto et al., 1989). To reduce this contamination, the tail current was measured 2.5 ms after the repolarization step. Because deactivation of I_{Ca} is very rapid and virtually complete in 1 ms (Yamamoto et al., 1989), no I_{Ca} should remain at this time. Also, the capacitive transient is largely over. As shown in Fig. 2, in spite of significant variations in individual cell currents (probably because of differences in cell size), the reversal potential is fixed at −84.2 mV. Since the expected Nernst potential for K^+ is −86.7 mV, the channel is highly selective to K^+. Thus, coupled with a sensitivity to blockade by Cs^+ and TEA (Yamamoto et al., 1989), This result indicates that the outward current is I_K.

Effect of $[Ca^{2+}]_o$ on I_K. Fig. 3 illustrates one case in which the I_K increased 4.2 times when $[Ca^{2+}]_o$ was increased from 3 to 30 mM. Similar increases were always observed in other cells, although the increase may only have been doubled. The possible mechanism underlying such stimulation will be dealt with in the Discussion,

but suffice it to mention here that in single-channel studies, there is evidence that an increase in the $[Ca^{2+}]_i$ is necessary to increase the probability of the K^+ channel being open (Hu et al., 1987b; footnote 1).[1]

Conversely, when $[Ca^{2+}]_o$ is reduced, or when I_{Ca} is blocked with Co^{2+}, I_K is reduced by $\sim 20\%$. In Fig. 1, the reduction is 25% for both the hump at 6 ms and
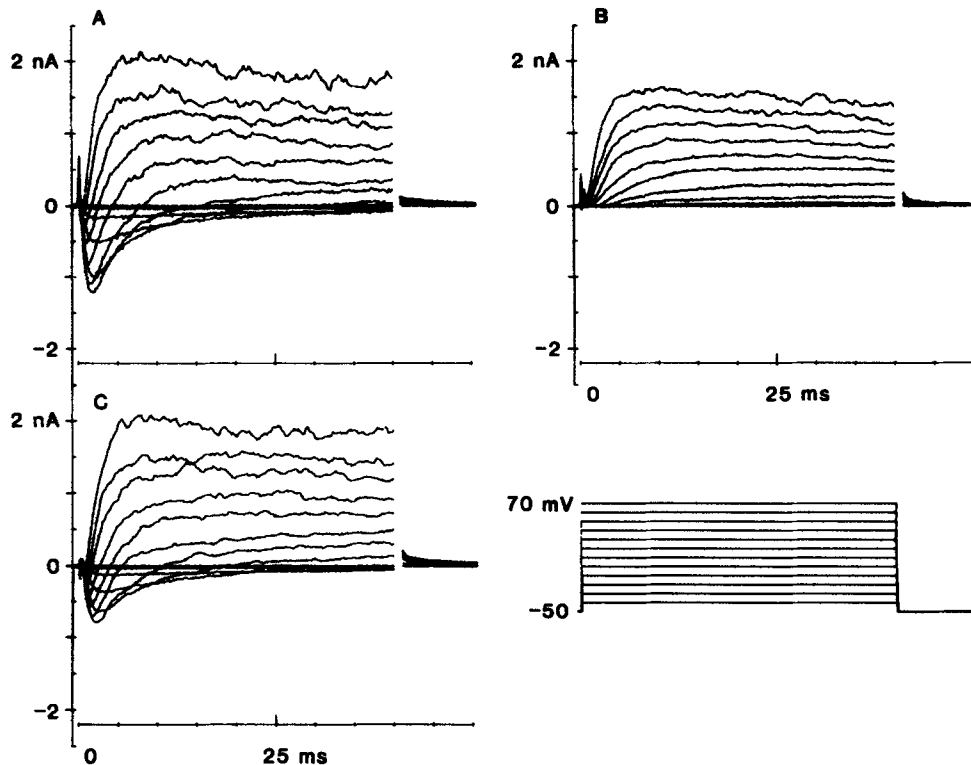

FIGURE 1. Use of Co^{2+} to isolate I_K. Cell capacitance, 53.3 pF. Series resistance was compensated for. $[Ca^{2+}]_o$ - 3 mM (solution C, Table I, Yamamoto et al., 1989). Holding potential, -50 mV; depolarizing steps in 10-mV increments to $+70$ mV. Temperature 34.4°C. (A) Net membrane current in 3 mM Ca^{2+}. (B) Membrane currents after the introduction of medium containing an additional 5 mM of Co^{2+}. Inward I_{Ca} is blocked, and outward current is lowered by 20–25%. (C) Membrane currents after a return to medium without Co^{2+}. Although I_{Ca} is smaller, possibly from rundown, outward current is virtually fully recovered.

the end of the 40-ms step. Ca^{2+}-free conditions are not desirable, because the selectivity of the Ca^{2+} channel is altered allowing other cations to pass outwards through it (Yamamoto et al., 1989) to interfere with an investigation of the I_K.

Co^{2+}-resistant I_K. The Co^{2+}-resistant component is readily analyzed because Co^{2+} is used to block the Ca^{2+} channel and thereby to isolate I_K. Fig. 4 summarizes

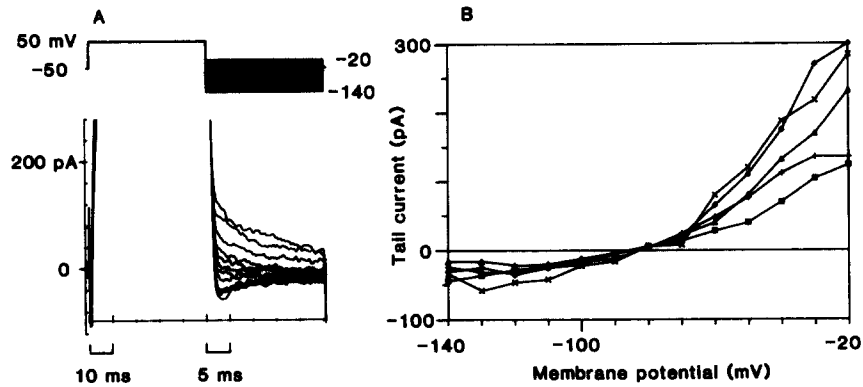[1] Hu, S. L., Y. Yamamoto, and C. Y. Kao., manuscript submitted for publication.

FIGURE 2. Estimation of potassium equilibrium potential. (A) Voltage protocol was used, and typical currents were from one cell. Capacitance, 50.6 pF; holding potential, -50 mV, depolarized to $+50$ mV, and then repolarized to various voltages as indicated. Note that time scales during depolarizing steps and during tail currents are different. $[Ca^{2+}]_o = 1$ mM. (B) Current-voltage relations of five individual cells, examined by a tail-current analysis similar to that shown in A. Cell capacitances are 50.6, 47.3, 61.4, 55.5, and 59.7 pF. In all five cells, current reversed between -90 and -80 mV. Reversal potential is -84.2 ± 0.6 mV (means $\pm$ SEM).
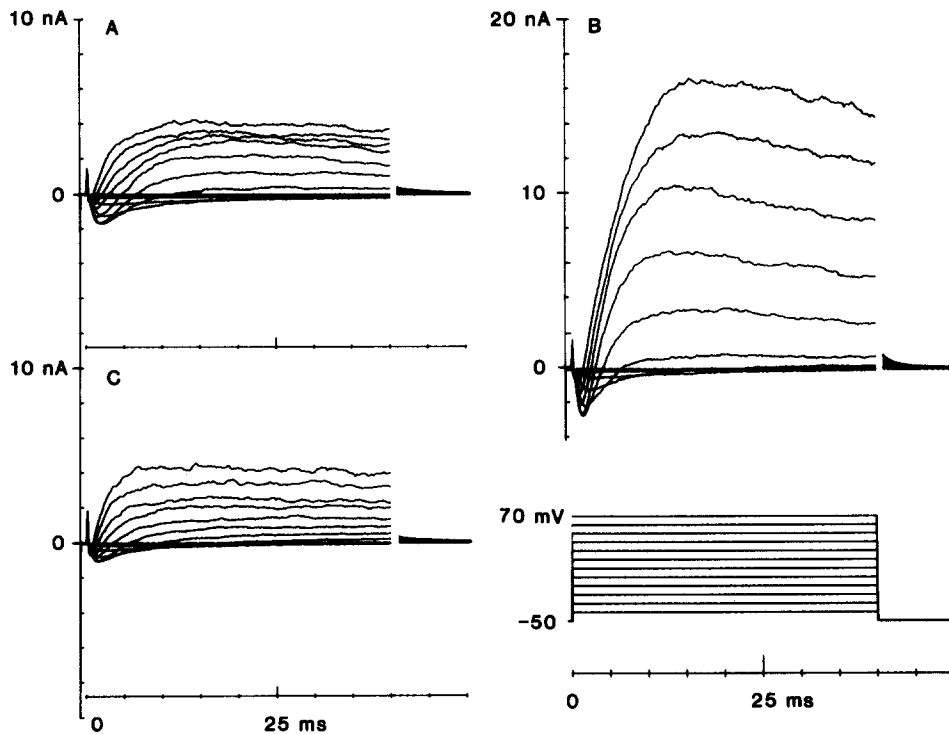

FIGURE 3. Effect of increasing $[Ca^{2+}]_o$ on membrane current. Cell capacitance, 89.7 pF; temperature, 32.6°C. Voltage protocol is shown in lower part of B. (A) Membrane currents in 3 mM Ca^{2+} (solution C). (B) Membrane currents in 30 mM Ca^{2+} (solution D). (C) Membrane currents in 3 mM Ca^{2+}, after B. Scale for current is same in all panels.

the results obtained on 10 cells. Fig. 4 *A* shows the typical Co^{2+}-resistant I_K of a single taenia myocyte in response to different depolarizing voltage steps. Fig. 4 *B* shows the normalized current-voltage relation as well as the conductance-voltage relation of 10 cells. It is evident that I_K above background noise can first be detected at ~ -20 mV. There is clear outward rectification up to 0 mV. Between 0 and 60
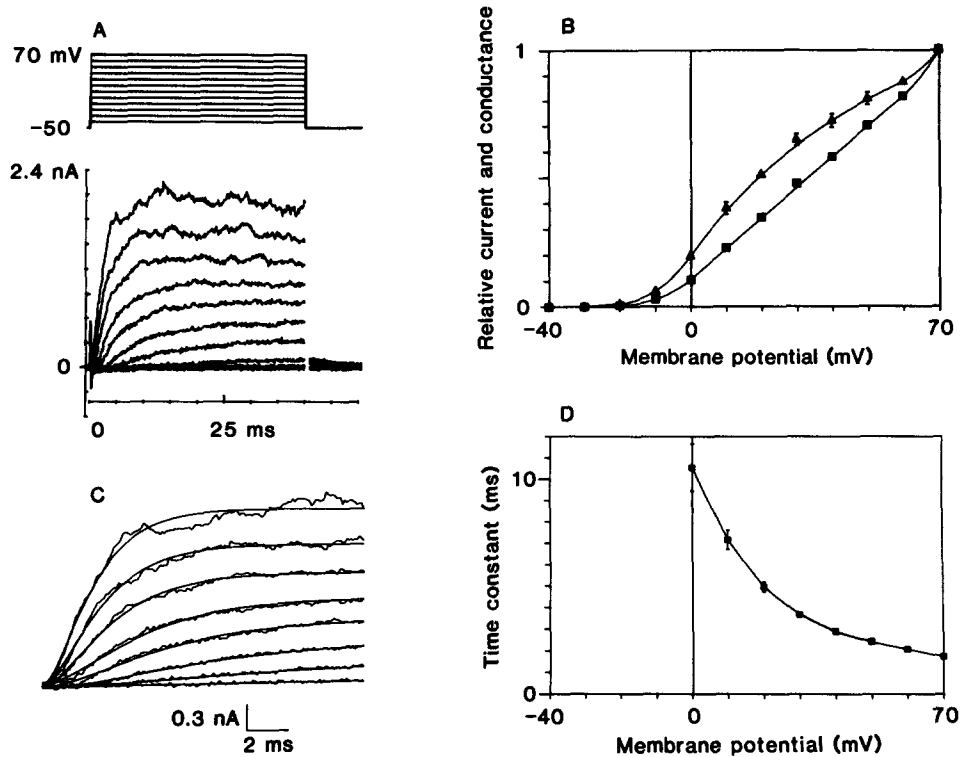

FIGURE 4. Activation of potassium current. (*A* and *C*) Current records from cell in 5 mM Co^{2+}. Cell capacitance, 65.7 pF. In *C*, the rising phase of I_K expanded on the fast time scale is shown. Noisy traces are recorded currents, at voltages between 0 and +70 mV, at every 10 mV. Smooth curves are fitted with $I = I_\infty [1 - \exp(-t/\tau)]^2$. (*B*) Current-voltage (squares) and conductance-voltage (triangles) relations of 10 cells. Currents were measured at the end of the test pulses. Data points are means ± SEM, each normalized to current at +70 mV. For obtaining chord conductances, the E_K used is -84.2 mV from data in Fig. 2. (*D*) Time constants of activation of 10 cells, shown as means ± SEM. Means are 10.6, 7.2, 5.0, 3.7, 2.9, 2.4, 2.1, and 1.7 ms from 0 to +70 mV.

mV, the *I-V* relation is linear, but more positive to 60 mV, outward rectification is again manifested. Although the linear portion might suggest that the current increments are due to increments in the driving force, the conductance-voltage curve shows that there is some increase in the conductance. Fig. 4, *C* and *D* show some features of the kinetics of activation that will be discussed in detail in a later section.

Ca^{2+}-activated I_K and its possible I-V relations. The Ca^{2+}-activated component of I_K is more difficult to isolate and must be examined in a more indirect way (Fig. 5). The cell whose current records are shown in Fig. 1 is used as an illustration. Fig. 5 Aa and Ba show the net currents of the cell in 3 mM of Ca^{2+} (solution C, Table I, Yamamoto et al., 1989). The current traces are identical to those in Fig. 1 A, but for clarity they have been separated into panel Aa for small depolarizations and Ba for larger depolarizations. The cell was then placed into 5 mM Co^{2+} in which the I_{Ca} was
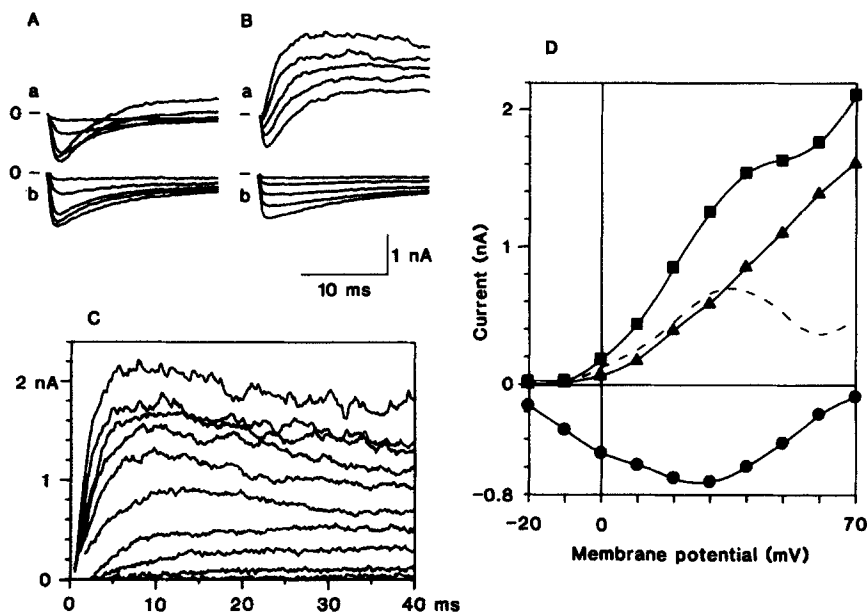

FIGURE 5.   Possible time course and magnitude of total I_K and its Ca^{2+}-activated component. (A and B) Current recordings in 3 mM Ca^{2+}. (Aa and Ba) Cell capacitance, 53.3 pF. Tracings are separated for clarity, (A) -20 to $+20$ mV; (B) $+30$ to $+70$ mV. The same cell was used as in Fig. 1. (Ab and Bb) Cell capacitance, 58.2 pF. The Cs^+ pipette solution blocked I_K. (C) Possible I_K in the net current recordings, obtained by subtracting I_{Ca} in Ab and Bb from net currents in Aa and Ba, at voltage steps of -20 to $+70$ mV. (D) Current-voltage relations of various currents. All currents are measured at 10 ms. Co^{2+}-resistant I_K (triangles), measured from the record shown in Fig. 1 B. I_K as derived in C (squares). The dashed line represents the difference between them, and may represent Ca^{2+}-activated I_K. I_{Ca} (circles) data points are taken from recordings in Ab and Bb, not at maximum, but at 10 ms to coincide with I_K measurements. Note that waxing and waning of Ca^{2+}-activated I_K mirrors that of I_{Ca}.

blocked (Fig. 1 B). The I-V relation of the Co^{2+}-resistant I_K is plotted as triangles in Fig. 5 D, in which all data points represent the current at 10 ms.

To sort out I_K from net currents, it is necessary to subtract any I_{Ca} from the traces of net current, and I_{Ca} can be isolated when Cs^+ is applied internally through the pipette solution (Yamamoto et al., 1989). What needs to be done is to record the net currents, using a K^+-based pipette solution, and then to change the pipette solution to a Cs^+-based solution to record only the I_{Ca}. We are unable at this time to change

the pipette solution during an experiment without compromising the quality of the electrode seal. For this reason, I_{Ca} was obtained from a surrogate cell amongst the many that had been studied (Yamamoto et al., 1989). The surrogate cell was selected by matching cell size, and the amplitude and the time course of decay of I_{Ca} at the -20- and -10-mV steps with those of the cell under study. The I_{Ca}'s of the surrogate cell are shown in Fig. 5, *Ab* and *Bb*, separated by size of depolarizations to avoid overlap of traces. Subtracting these I_{Ca}'s from the net currents in *Aa* and *Ba* leads to possible I_K's which are shown in Fig. 5 *C*. Use of a surrogate is always attended by possible errors; therefore, we did not attempt to make any detailed analysis of the time course of the derived I_K (Fig. 5 *C*).

Instead, for discussion, we took only the value at 10 ms, and showed them in a possible *I-V* relation of the total I_K (square symbols in Fig. 5 *D*). If this curve were
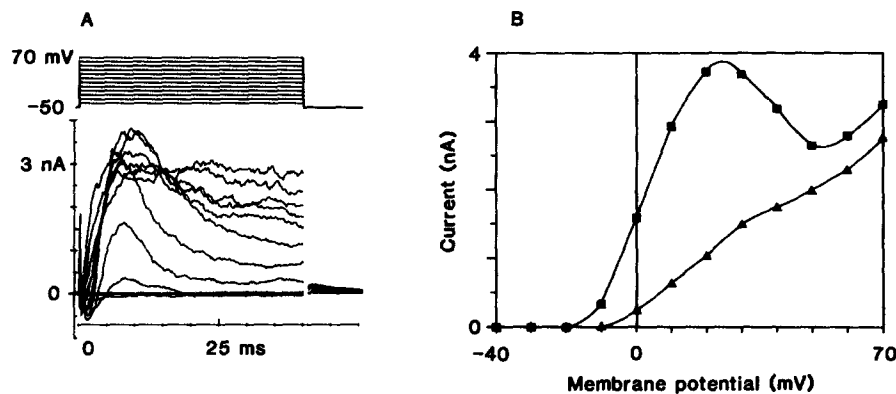

FIGURE 6.   Peak and late outward currents and their *I-V* relations. Cell capacitance, 52.3 pF; temperature, 32.5°C. $[Ca^{2+}]_o = 1$ mM (solution B). Pipette solution contains 0.5 mM EGTA (half of usual). Series resistance was compensated for. (*A*) Membrane currents. Note extreme humpiness of outward current and rapid decline towards stable level. (*B*) Current-voltage relations at peak of outward current (squares) and at 40 ms (triangles).

representative of the total I_K, then the difference between it and the *I-V* relation of the Co^{2+}-resistant I_K should represent the *I-V* relation of the Ca^{2+}-activated component of the I_k, which is shown as the dashed curve in Fig. 5 *D*. To correlate this curve with potential intracellular $[Ca^{2+}]$, I_{Ca} values (Fig. 5, *Ab* and *Bb*) were measured, not at the peak but isochronally with I_K at 10 ms. From Fig. 5 *D*, it is apparent that there is much mirrored coincidence between the I_{Ca} and the Ca^{2+}-activated I_K.

Fig. 6 illustrates an infrequent, but potentially significant, observation in which a taenia myocyte was clamped with a pipette solution containing half the usual concentration of EGTA (0.5 instead of 1 mM). The bath solution contained 1 mM Ca^{2+} and no Co^{2+} (solution B, Table I of Yamamoto et al., 1989). An inward I_{Ca} of ~ 0.6 nA was first seen, followed by an I_K that exhibited a prominent hump before decaying to a steady level by ~ 35 ms. The series resistance was relatively low, and $\sim 70\%$ of it was compensated; the voltage error owing to series resistant is estimated to be < 3 mV even when 3.8 nA of I_K was registered. Thus, the hump is probably due to

some Ca^{2+}-activated I_K. In Fig. 6 B, the I-V relations of the peak outward current and also at the end ot the 40-ms pulse are plotted. The prominence of the N-shaped segment may have been the result of the lowered EGTA in the cell.

Activation and deactivation. Measurable levels of I_K are first detected at ~ −20 mV (Fig. 4). The rate of activation is strongly voltage-dependent. In Fig. 4 C, traces of I_K of a representative cell are shown to be well fitted by n^2 kinetics. The time constant of activation, averaged from 10 cells, falls from 10.6 ms at 0 mV to 1.74 ms at +70 mV (Fig. 4 D).

Deactivation of I_K is much slower than that of I_{Ca} and occurs over tens of milliseconds (e.g., Fig. 2 A). Although analysis was not easy because of the small sizes of the tail current, the time course of decay can be roughly fitted with a single exponential function. Fig. 7 summarizes the averaged time constants of decay at −50, −40,
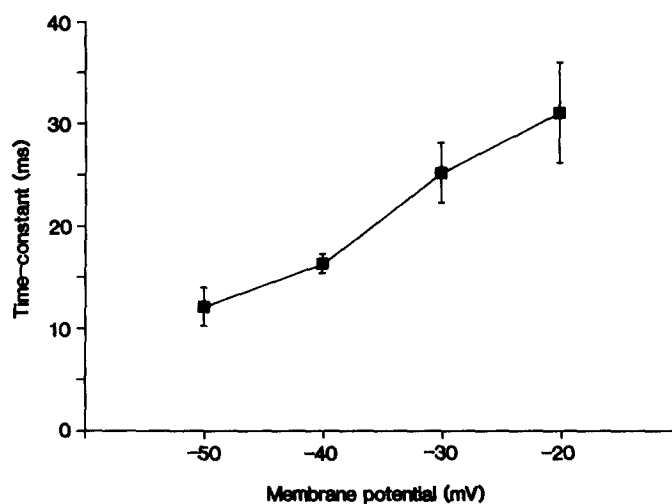

FIGURE 7. Deactivation of potassium current. Time-constants of decay of tail current (as illustrated in Fig. 2 A) of five individual cells. Data points are means; vertical bars represent SEM.

−30, and −20 mV of five individual taenia myocytes. Within this narrow range, the average time constant of decay decreases monotonically with increasing negativity.

Inactivation

Kinetics. As is evident from the current records (e.g., Figs. 1 B and 4 A), Co^{2+}-resistant I_K declines somewhat even when the voltage step was maintained, especially at large depolarizations. This phenomenon is most likely caused by some inactivation (see e.g., Klöckner and Isenberg, 1985). To examine this process in more detail, several cells in Co^{2+}-containing solution were subjected to command voltage steps of 4.5-s duration. Fig. 8 A shows that even though I_K declines appreciably over this period, there is a residual noninactivating component at the end (if it inactivates, it does so at a rate too slow to be detected during the 4.5-s step). Figure 8 B shows that the inactivation time course in individual cells can be reasonably well fitted by two exponential terms. In five cells, the relation of membrane voltage to the time
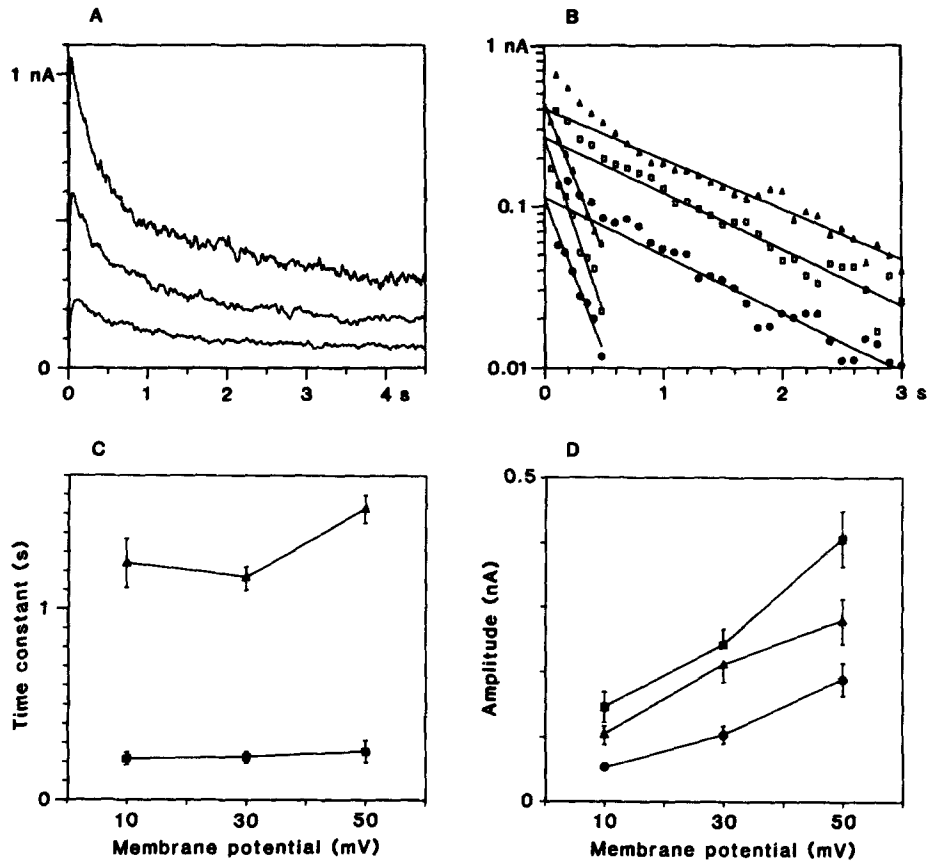
FIGURE 8. Inactivation of Co^{2+}-resistant I_K. (A) I_K produced by depolarizing to +10 mV (bottom trace), +30 mV (middle), and +50 mV (top), using a 4.5-s step. Cell capacitance, 65.7 pF. Note the decline of I_K, and the persistence of some noninactivating current. (B) Time course of inactivation in the same cell, plotted on semilogarithmic coordinates. For current at each voltage (represented by filled circles at +10 mV, squares at +30 mV, and triangles at +50 mV), the time course can be resolved into two exponential (fast and slow) and noninactivating components. Fit:

$$+10 \text{ mV:} I = 0.073 + 0.112 \exp(-t/0.229) + 0.113 \exp(-t/1.213)$$
$$+30 \text{ mV:} I = 0.165 + 0.269 \exp(-t/0.197) + 0.270 \exp(-t/1.244)$$
$$+50 \text{ mV:} I = 0.303 + 0.441 \exp(-t/0.233) + 0.404 \exp(-t/1.388)$$

(C) Time constants of inactivation of fast (squares) and slow (triangles) components; means ± SEM of six cells. (D) Amplitude of fast (squares), slow (triangles) and noninactivating (circles) components. The amplitude obtained as y intercept of each component in semilog plots is similar to that in B.

constant of decay and amplitude have been averaged (Fig. 8, C and D). The faster component decays independently of voltage between +10 and +50 mV, with a time constant of $\sim$ 240 ms. The slower component also decays independently of membrane voltage between +10 and +30 mV with a time constant of $\sim$ 1.2 s, but at +50 mV, the decay is significantly slower, with an average time constant of 1.5 s.
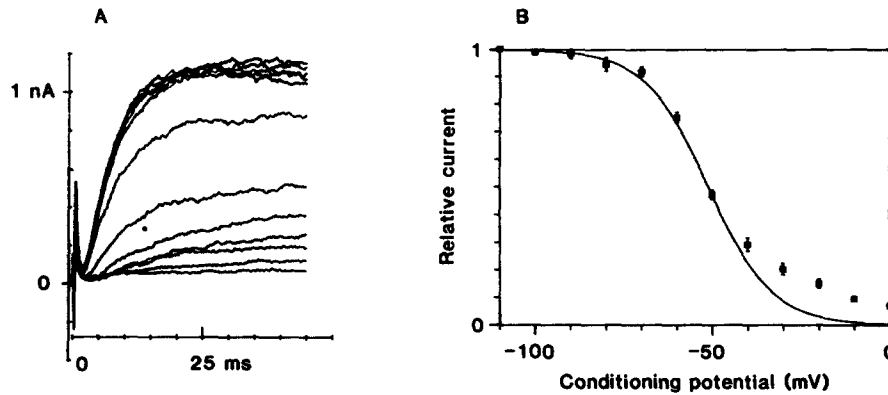
FIGURE 9. Steady-state inactivation of Co^{2+}-resistant potassium current. (*A*) Typical current records. Currents were activated by depolarizing to +10 mV, preceded by a conditioning step of 10-s duration at different voltages between −110 and 0 mV, in 10-mV increments. Currents recorded during the conditioning pulse are not shown. (*B*) Relative current amplitude vs. conditioning potential. Data points are means of eight cells, vertical bars are SEM if larger than symbol. For each cell, current has been normalized to that at −110 mV conditioning potential (1.0). Smooth curve is $y = \{1 + \exp[(V + 51.0 \text{ mV})/9 \text{ mV}]\}^{-1}$. Note non-inactivating component.

Steady-state inactivation. This was studied in eight cells in Co^{2+}-containing solution, using the usual two-pulse method (Fig. 9). The conditioning pulse (V1) ranged from −110 to 0 mV, and was 10 s long. The test pulse (V2), following V1 without any interval, was constant to +10 mV, and was 45 ms long. The steady-state inactivation of I_K generally follows a sigmoidal shape with respect to voltage, but unlike the classical curve, it is not symmetrical. As can be seen in Fig. 9 *B*, a smooth curve following Boltzman distribution, with half-inactivation at −51 mV and a slope of 9 mV covers all points negative to −50 mV. Positive to −40 mV, all points consistently exceed the theoretical curve, possibly suggesting the existence of two or more populations of K^+ channels with different h_∞ properties.
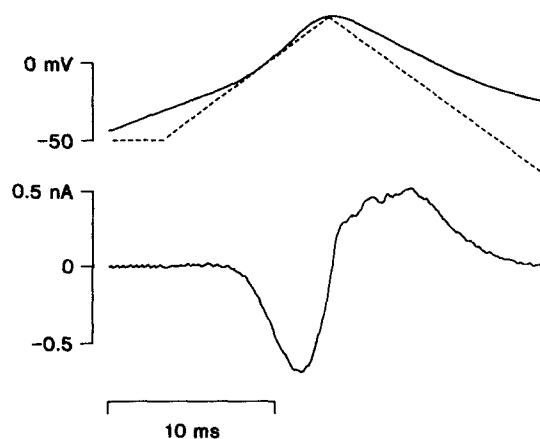

FIGURE 10. Membrane current during a ramp clamp. $[Ca^{2+}]_o = 3$ mM. Top trace, action potential elicited by brief current pulse; cell capacitance, 49.1 pF. Middle trace in broken line, ramp voltage command structured to mimic action potential. Bottom trace, current due to ramp command. Cell capacitance, 52.8 pF. Note that outward current coincides with the repolarization phase of action potential.

Outward current during a ramp clamp. In a qualitative way, the question of whether activation of I_K participates in the repolarization of an action potential under physiological conditions is examined by using a ramp-clamp experiment. A ramp command was constructed to mimic the action potential of a taenia cell that had been elicited by a brief current pulse. The ramp was then used to clamp another taenia cell, and the net current, including both inward and outward currents, were recorded (Fig. 10). It is evident that a substantial amount of outward current coincides with the repolarizing phase of the action potential.

DISCUSSION

Potassium Equilibrium Potential and Selectivity

In earlier work on the multicellular preparations of the taenia coli (Inomata and Kao, 1976), K^+ had been identified as the charge carrier, and the reversal potential of that current (termed E_b) was estimated to be 15–20 mV more negative than the resting potential. At a usual holding potential (also usual resting potential) of -50 mV (Inomata and Kao, 1976), the reversal potential, chiefly E_K, would have been ~ -65 to -70 mV. These values are substantially lower than the E_K of -84 mV determined in the present experiments. Several reasons can account for the difference. In the multicellular preparations, the intracellular $[K^+]$ was not accessible to experimental control. The lower reversal potential could be caused by a lower $[K^+]_i$ in those cells, an accumulation of K^+ in the extracellular clefts to raise $[K^+]_o$, a reduced selectivity to K^+, or, most likely, a combination of these causes. In the dispersed single cells, the cell interior rapidly equilibrates with the pipette solution. Thus, the $[K^+]_i$ is the same as that in the pipette, and maintained constant. There is no extracellular clefts for accumulating any K^+. Therefore, it is not surprising that the E_K found here is very close to the theoretically expected value.

Ca^{2+} Dependence of I_K

The fact that I_K is reduced when Co^{2+} is used to block I_{Ca} suggests that influxed Ca^{2+} has a role in activating I_K. Ca^{2+}-activated potassium channels have been found in many types of cells (for summary, see Hille, 1984). Among smooth muscle cells, the presence of a Ca^{2+}-activated K^+ conductance has been intimated before on multicellular preparations of the guinea pig taenia coli (Inomata and Kao, 1979, 1985). Ca^{2+}-activated potassium channels have been found in single-channel recordings in smooth muscle cell patches of the following preparations: toad stomach muscle (Singer and Walsh, 1987a, b), rabbit jejunal muscle (Benham et al., 1986), rabbit portal vein muscle (Inoue et al., 1985, 1986), and the guinea pig taenia coli (Hu et al., 1987a, b).

A difficult problem in whole-cell recordings is to know the true magnitude and time course of the I_K. As mentioned, the use of Co^{2+} introduces a systematic error by depressing some I_K. On the other hand, in records of total membrane currents, there is too much temporal overlap of the inward and outward currents for any reliable determination of I_K. Fig. 5 illustrates an attempt to separate I_K from the net current recordings by subtracting I_{Ca}. For reasons detailed in the Results, the procedure adopted is the best available to us at the present time, and, in spite of some

reservations, the outcome is reasonably indicative of the trends. The I-V relation of the derived I_K is N-shaped with a distinct kink, a characteristic that is also seen in other cells with Ca^{2+}-activated I_K (molluscan neuron, Hermann and Gorman, 1979; Gorman and Thomas, 1980; guinea pig urinary bladder muscle, Klöckner and Isenberg, 1985; and toad stomach muscle, Walsh and Singer, 1987). If the Co^{2+}-resistant I_K were representative primarily of the voltage-dependent potassium conductance, then the difference between it and the total I_K might be thought of as representing that part of the potassium conductance activated by a surge in the intracellular Ca^{2+}.

In most of our experiment, 1 mM EGTA is incorporated in the pipette solution. Because the intracellular environment rapidly equilibrates with the pipette solution upon rupture of the cell membrane, it can be assumed that the free Ca^{2+} concentration in the cell is kept very low. Since no contractions were seen in our experiments, the intracellular free Ca^{2+} concentration was probably below the threshold for contraction in taenia cells (10^{-8} M, Obara and Yamada, 1984). When Ca^{2+}-activated I_K can be seen under such circumstances, it probably can be seen in conditions when the Ca^{2+} buffering is less efficient. Thus, in the few experiments in which 0.5 mM EGTA was used in the pipette solution, the hump in I_K associated with the Ca^{2+}-activated component was markedly more prominent than in those cases with 1 mM EGTA (Fig. 6). Under physiological conditions, when $[Ca^{2+}]_i$ could rise to micromolar concentrations, the Ca^{2+}-activated I_K must be very substantial. Such an expectation is supported by the observation that in some single-channel recordings, the probability of opening of an identified delay rectifier channel is greatly enhanced by increased $[Ca^{2+}]_i$ (Hu et al., 1987a; see footnote 1).

Voltage-dependence of I_K

Although our results have shown that there are two components in the I_K of the taenia myocytes, a $[Ca^{2+}]_i$-dependent component and a Co^{2+}-resistant, voltage-dependent component, the question of whether these properties arise from a single population of K^+ channels or from different populations, each with a single component, remains unresolved. Ca^{2+}-activated I_K can also be voltage dependent (e.g., Gorman and Thomas, 1980; Pallotta et al., 1981; Barrett et al., 1982; Latorre et al., 1982). In the taenia myocytes, there are three types of K^+ channels (Hu et al., 1987a; see footnote 1). The predominant type has a single-channel conductance of 150 pS, and is probably the delayed rectifier channel. It is both voltage dependent and highly sensitive to $[Ca^{2+}]_i$.

Activation and Deactivation

As shown in Fig. 4, activation of the Co^{2+}-resistant I_K in the taenia cell is well described by n^2 kinetics. Although differing significantly from the better-known n^4 kinetics (such as that in the squid giant axon), n^2 kinetics is not unique. In the node of Ranvier of the *Xenopus* myelinated nerve, Frankenhaeuser (1963) has described such a process. That deactivation of I_K can be approximated by a single exponential rate that is voltage sensitive probably reflects the predominant contribution of a single population of K^+ channels to the delayed rectifier current.

Inactivation

During a maintained depolarization, the Co^{2+}-resistant I_K inactivates with two exponential components, leaving a small fraction of noninactivating component. The noninactivating component is also seen in the steady-state inactivation curve (Fig. 9). Rather similar features have been described for the I_K in the *Xenopus* myelinated nerve (Schwarz and Vogel, 1971). These observations could be due to multiple forms of K^+ channel, which have been observed in single-channel recordings of the taenia mycoytes (Hu et al., 1987a; see footnote 1). However, aside from an identification of the 150-pS channel as the delayed rectifier, we have no evidence to link the slowly inactivating or the noninactivating components with any type of single K^+ channels.

In the steady-state inactivation relation (Fig. 9), it has been shown that at the usual resting potential of -50 mV, only half of the K^+ channels are available. The cells used for these studies were in Co^{2+}-containing solution, and a significant portion of the potassium conductance, the Ca^{2+}-activated component, had already been removed. Under physiological conditions, when the Ca^{2+}-activated potassium conductance functions actively, sufficient outward current can no doubt be generated to cause repolarization of the action potential (e.g., Fig. 10). The role of the Ca^{2+}-activated I_K may also account for an observation that in Sr^{2+}, the repolarization seems to be more dependent on the rate of inactivation of the early inward current than on I_K (Inomata and Kao, 1979), because Sr^{2+} not only slows the inactivation of the early inward current, but it is also less effective in stimulating the Ca^{2+}-activated I_K.

REFERENCES

Barrett, J. N., K. L. Magleby, and B. S. Pallotta. 1982. Properties of single calcium-activated potassium channels in cultured rat muscle. *Journal of Physiology.* 331:211–230.

Benham, C. D., T. B. Bolton, R. J. Lang, and T. Takewaki. 1986. Calcium-activated potassium channels in single smooth muscle cells of rabbit jejunum and guinea-pig mesenteric artery. *Journal of Physiology.* 371:45–67.

Frankenhaeuser, B. 1963. A quantitative description of potassium currents in myelinated nerve fibers of *Xenopus laevis*. *Journal of Physiology.* 169:424–430.

Gorman, A. L. F., and M. V. Thomas. 1980. Potassium conductance and internal calcium accumulation in a molluscan neuron. *Journal of Physiology.* 308:287–313.

Hermann, A., and A. L. F. Gorman. 1979. Blockade of voltage-dependent and Ca^{2+}-dependent K^+ current components by internal Ba^{2+} in molluscan pacemaker neurons. *Experientia.* 35/2:229–231.

Hille, B. 1984. Ionic Channels of Excitable Membranes. Sinauer Associates Inc., Sunderland, MA. 104–109.

Hu, S. L., Y. Yamamoto, and C. Y. Kao. 1987a. Single-channel basis of delayed rectification in dispersed cells of guinea pig taenia coli. Biophysical Journal. 51:200a. (Abstr.)

Hu, S. L., Y. Yamamoto, and C. Y. Kao. 1987b. Selectivity of the single delayed rectifier channel in smooth muscle cells of the guinea pig taenia coli. Federation Proceedings. 46:507. (Abstr.)

Inomata, H., and C. Y. Kao. 1976. Ionic currents in the guinea pig taenia coli. Journal of Physiology. 255:347–378.

Inomata, H., and C. Y. Kao. 1979. Ionic mechanisms of repolarization in the guinea-pig taneia coli as revealed by the actions of strontium. Journal of Physiology. 297:443–462.

Inomata, H., and C. Y. Kao. 1985. Actions of Ba^{2+} on ionic current of the guinea-pig taenia coli. Journal of Pharmacology and Experimental Therapeutics. 233:112–124.

Inoue, R., K. Kitamura, and H. Kuriyama. 1985. Two Ca-dependent K-channels classified by the application of tetraethylammonim distribute to smooth muscle membranes of the rabbit portal vein. Pflügers Archiv. 405:173–179.

Inoue, R., K. Okabe, K. Kitamura, and H. Kuriyama. 1986. A newly identified Ca^{2+}-dependent K^+ channel in the smooth muscle membrane of single cells dispersed from the rabbit portal vein. Pflügers Archiv. 406:138–143.

Klöckner, U., and G. Isenberg. 1985. Action potentials and net membrane currents of isolated smooth muscle cells (urinary bladder of the guinea pig). Pflügers Archiv. 405:329–339.

Latorre, R., C. Vergara, and C. Hidalgo. 1982. Reconstitution in planar lipid bilayers of Ca^{2+}-dependent K^+ channel from transverse tubule membranes isolated from rabbit skeletal muscle. Proceedings of the National Academy of Sciences. 79:805–809.

Obara, K., and T. Yamada. 1984. Some properties of chemically skinned single smooth muscle cells. Japanese Journal of Physiology. 34:1089–1104.

Pallotta, B. S., K. L. Magleby, and J. N. Barrett. 1981. Single channel recordings of Ca^{2+}-activated K^+ currents in rat muscle cell culture. Nature. 293:471–474.

Schwarz, J. R., and W. Vogel. 1971. Potassium inactivation in single myelinated nerve fibres of Xenopus laevis. Pflügers Archiv. 330:61–73.

Singer, J. J., and J. V. Walsh. 1987a. Characterization of calcium-activated potassium channels in single smooth muscle cells using the patch-clamp technique. Pflügers Archiv. 408:98–111.

Singer, J. J., and J. V. Walsh. 1987b. Large-conductance Ca^{2+}-activated K^+ channels in freshly dissociated smooth muscle cells. Membrane Biochemistry. 6:83–110.

Walsh, J. V., and J. J. Singer. 1987. Identification and characterization of major ionic currents in isolated smooth muscle cells using the voltage-clamp technique. Pflügers Archiv. 408:83–97.

Yamamoto, Y., S. L. Hu, and C. Y. Kao. 1989. The inward current in single smooth muscle cells of the guinea pig taenia coli. Journal of General Physiology. 93:521–550.